Published in final edited form as:
J Immunol. 2012 June 1; 188(11): 5421–5427. doi:10.4049/jimmunol.1200242.

Stathmin regulates microtubule dynamics and MTOC polarization in activated T cells

Erin L. Filbert[*,¶], **Marie Le Borgne**[*,§,¶], **Joseph Lin**[*,‡], **John E. Heuser**[†], and **Andrey S. Shaw**[*,§]

[*]Department of Pathology and Immunology, Washington University School of Medicine, 660 South Euclid, Saint Louis, Missouri 63110, USA

[†]Department of Cell Biology, Washington University School of Medicine, 660 South Euclid, Saint Louis, Missouri 63110, USA

[‡]Current address: Department of Biology, Sonoma State University, 1801 East Cotati, Rohnert Park, CA 94928, USA

[§]Howard Hughes Medical Institute, Washington University School of Medicine, 660 South Euclid, Saint Louis, Missouri 63110, USA

Abstract

Polarization of T cells involves reorientation of the microtubule-organizing center (MTOC). Because activated ERK is localized at the immunological synapse, we investigated its role by showing that ERK activation is important for MTOC polarization. Suspecting that ERK phosphorylates a regulator of microtubules, we next focused on stathmin, a known ERK substrate. Our work indicates that during T cell activation, ERK is recruited to the synapse allowing it to phosphorylate stathmin molecules near the immunological synapse. Supporting an important role of stathmin phosphorylation in T cell activation, we showed that T cell activation results in increased microtubule growth rate dependent on the presence of stathmin. The significance of this finding was demonstrated by results showing that CTL from stathmin−/− mice displayed defective MTOC polarization and defective target cell cytolysis. These data implicate stathmin as a regulator of the microtubule network during T cell activation.

Introduction

An early step in the activation of T cells is the polarization of the cell. This is demonstrated by the formation of the immunological synapse at the contact surface between the T cell and the antigen presenting cells (1). At the same time, the microtubule-organizing center (MTOC) moves from a position in the trailing uropod of the migrating T cell to a new position between the nucleus and the immunological synapse (2–5). T cell polarization directs intracellular trafficking of vesicles, facilitates the formation of the synapse and directs the polarized secretion of cytokines and cytolytic granules important in cell lysis (4, 6, 7).

While the importance of MTOC repositioning in T cell activation is clearly important, the mechanism of its reorientation is less clear. Consistent with a requirement for T cell signaling, it was previously shown that molecules downstream of the TCR like Lck, Zap70, Lat, SLP76, PI3K and PLC-γ are all important for MTOC reorientation to the immune

Corresponding author: Andrey S. Shaw, MD Department of Pathology & Immunology/HHMI Washington University School of Medicine, St. Louis, MO 63110 tel: 314-362 4614 ; fax: 314-362-9108 ashaw@wustl.edu.
[¶]Authors contributed equally to this work.

synapse (8–11). Recently, it was shown that accumulation of diacylglycerol (DAG) is sufficient to induce MTOC polarization (10, 12). While dynein and the PKC isozymes θ, η and ε appear to be important for this process, the exact mechanism explaining how DAG induces MTOC reorientation is not known. Nonetheless, these data demonstrate that local signaling events at the immune synapse lead to reorganization of the microtubule network.

Interestingly, one of the most important effectors of DAG is RAS-GRP, the GTP exchange factor that functions to activate RAS and subsequently the ERK-MAPK pathway (13). A number of studies have shown that active ERK accumulates at the immune synapse (14, 15) and that ERK activation is also thought to be important for MTOC polarization in T cells (16–18). Consistent with an important role for ERK in T cell polarization, cytolytic activity mediated by CTLs and NK cells is inhibited with ERK inhibition (16, 17). In addition, NK cells lacking the ERK-MAPK scaffold KSR1, which is required for the localization of ERK to the immune synapse, also fail to polarize their granules and kill target cells poorly (14).

Here we investigated the potential role of ERK in MTOC reorientation. After confirming that ERK is required for MTOC polarization, we hypothesized that a specific substrate of ERK might be a regulator of the microtubule cytoskeleton. Because it is a known ERK substrate (19–23), we focused on the microtubule binding protein, stathmin (OP18), as a possible link between ERK and the microtubule cytoskeleton. The stathmin family of proteins is highly conserved and functions by binding to free tubulin heterodimers in the cytoplasm and thereby regulates the concentration of free tubulin (24). Phosphorylation of stathmin by a number of serine-threonine kinases, including ERK, results in release of bound tubulin heterodimers and enhanced polymerization of the microtubule network.

Although stathmin was originally characterized as an oncoprotein over-expressed in T leukemia cells (25), little is known about its function in developing and mature T cells (26). Previous studies verify that it becomes phosphorylated after TCR stimulation but the biological outcome in T cell activation is not known (27–29). Analysis of stathmin-deficient mice showed a reduction in thymocyte cellularity and peripheral T cell numbers, but additional immune cell analyses were not reported (30).

We found that stathmin is rapidly phosphorylated downstream of the T cell receptor and that phosphorylated stathmin is localized to the immune synapse. Consistent with the importance of ERK localization at the synapse, T cells lacking the MAPK scaffold KSR1 showed defects in stathmin localization. This was important for MTOC polarization as we found that microtubule growth rates were slowed in the absence of stathmin resulting in a delay of MTOC reorientation and defects in CTL cytolysis. These data are the first to implicate stathmin in the regulation of microtubule dynamics in activated T cells.

Materials and Methods

Mice

Stathmin knockout mice on a C57/B6J background have been previously described (30) and were a generous gift from Dr. Gleb Shumyatsky (Rutgers University). Stathmin−/− mice were crossed with OT-1 TCR (31) and AND TCR (32) transgenic mice. Age and gender-matched stathmin wild-type or heterozygous littermate controls were used for all experiments. KSR1 knockout mice on a C57/B6J background were previously described (33) and were crossed to AND TCR transgenic mice. All mice were housed under specific pathogen-free conditions in the Washington University animal facilities in accordance with institutional guidelines.

Cell Culture and Antibodies

EL-4, RMA-S, CH27 and Jurkat cells were maintained in RPMI 1640 supplemented with 10% FBS, 2 mM glutamine. T cells isolated from OT-1 or AND TCR transgenic mice T cells were cultured in IMDM supplemented with 10% FBS, 2 mM glutamine, nonessential amino acids, sodium pyruvate, 2-ME, penicillin, and streptomycin. TCR stimulation was performed with anti-mouse CD3 (2C11) and anti-mouse CD28 (37.51) or anti-human CD3 (OKT3). Anti-stathmin (O0138), anti-α-tubulin (FITC conjugated) and anti-ppERK antibodies were from Sigma. Anti-phosphoS24-stathmin (ab47398) was from Abcam. ERK2 and PKCθ antibodies were from Santa Cruz. PLC-γ1 and p-PLC-γ1 antibodies were from Cell Signaling Technology. Anti-mouse CD107a-PE (1D4B) and ant-mouse CD8-FITC (53-6.7) were from BD Bioscience. All secondary antibodies were from Jackson ImmunoResearch Laboratories. CFSE and CMTPX dyes used for APC labeling in some experiments were obtained from Molecular Probes. All inhibitors were purchased from Sigma-Aldrich.

Western Blot

Jurkat or primary mouse T cells were starved for 1 h in RPMI 1640. Cells were stimulated with PMA/ionomycin or anti-TCR antibody in suspension for the indicated time points. After stimulation, the pellet was re-suspended in ice-coldlysis buffer (0.1 M Tris base, 140 mM NaCl, 1 mM EDTA, 1% NP-40,1 mM phenylmethylsulfonyl fluoride, 1 mM sodium orthovanadate, and 50 mM sodium fluoride). After centrifugation, proteins from cell lysates were resolved by sodium dodecyl sulfate-polyacrylamidegel electrophoresis (SDS-PAGE) and analyzed by immunoblotting with the indicated primary antibodies followed by incubationanti-rabbit or anti-mouse IgG coupled to horseradish peroxidase. ECL western blotting substrate (Pierce) was used for detection. Band intensity for quantification was measured using ImageJ.

Immunoflorescence Assays

OT-1 and AND T cell conjugates were made by loading RMA-S or EL-4 cells with 1 μM SIINFEKL peptide, and CH27 cells with 1 μM MCC (88-103) peptide, respectively, overnight at 37°C, before mixing with OT-1 or AND T cells at a 1:1 ratio. Cells were pelleted by brief centrifugation and incubated at 37°C for 5-10 min. Conjugates were gently re-suspended and allowed to settle on poly-L-lysine-coatedslides before fixation in 2% paraformaldehyde (PFA). Cells were then permeabilized with 0.1% Triton X-100 and stained with the indicated antibodies. For polarization toward anti-TCR, coverslips were coated with anti-CD3 +/− anti-CD28 antibody and cells pretreated or not for 1 hour with indicated inhibitors (eg. UO126, RPcAMP and cytochalasin D) were allowed to settle on to the coverslips before fixation in 2% PFA. Polarization toward the coverslip was scored blinded. Cells were considered polarization positive if the MTOC was clearly visible and it was centrally located within the cell in the focal plane adjacent to the coverslip. All images were collected on an Olympus FV1000 with 60x objective.

In Vivo Migration Assay

Naive T cells were purified from spleen and lymph nodes of stathmin wild-type or knockout mice, labeled with either CFSE or CMTPX dye and injected at a 1:1 ratio into the footpad of congenic mice stimulated 16 hours prior with 1μg LPS. Popliteal lymph nodes were harvested after 3 hours, made into a single-cell suspension and donor T cell migration was assessed by flow cytometry.

Proliferation Assay

Rested T cells from stathmin wild-type or knockout spleen and lymph nodes were stimulated for 48 hr with the indicated concentrations of plate-bound anti-CD3/CD28 or PMA/ionomycin, pulsed with 1 μCi of [^{3}H] thymidine/well, harvested after 16 hours, and scintillation counted.

Cytokine Production Measurements

OT1 T cells activated *in vitro* for 5 days were stimulated with soluble anti-CD3/CD28-biotin + streptavidin at 37°C. Supernatants were collected after 18 hrs. Detection of IFN-γ in supernatants was obtained using CBA Flex Sets (BD Biosciences) and analysis on a FACS Canto II (BD Biosciences).

Measurement of Intracellular Calcium

T cells activated *in vitro* for 5 days were loaded with 1 μM of the calcium detection dye Fura-2 (Invitrogen) for 30 min at 37°C in calcium buffer (135 mM NaCl, 5 mM KCl, 1 mM $CaCl_2$, 1mM $MgCl_2$, 5.6 mM glucose, 10 mM Hepes, 0.1% BSA), plated on a poly-L-Lysine coated 96-well plate, and washed twice in buffer free calcium. Fluorescence ratio between 340 nm and 380 nm excitation at 510 nm emission was recorded using a Flexstation. Cells were stimulated after 30 sec with anti-CD3-biot + anti-CD28-biot (5 mg/mL of each) + streptavidin (20 mg/mL), and $CaCl_2$ was added after 330 sec (1 mM final concentration). Data are represented as changes in 340/380 ratio compared with the baseline.

Cytolysis Assay

Splenocytes from stathmin wild-type (littermate controls) or knockout OT-1 TCR transgenic mice were stimulated by the addition of 1μM SIINFEKL peptide for 5 days to generate CTL. A standard ^{51}Cr-release assay was performed. Briefly, ^{51}Cr-labeled target cells pulsed with SIINFEKL were plated in 96-well U-bottom plates (10,000 cells/well) with CTL at varying E:T cell ratios and cultured for 4-6h at 37°C. The supernatants were then collected and readon a MicroBeta counter (PerkinElmer). Specific lysis was calculated as follows: [(avg sample cpm − avg spontaneous cpm) / (avg max cpm – avg spontaneous cpm)] x 100.

Degranulation Assay

OT1 T cells activated *in vitro* for 5 days were resuspended in complete media with 10% FCS together with target cells (RMA-S or EL-4) previously loaded with 1 μM SIINFEKL peptide. The cells were incubated at 37°C for 45 min in the presence of 5 mg/mL of anti-CD107a (LAMP-1)-PE antibody. Cells were then washed and stained at 4°C with anti-mouse CD8 antibody and analyzed on a FACS Calibur (BD Biosciences).

Microtubule Growth Rate Measurements

Whole spleens from stathmin wild-type (littermate controls) or knockout mice were activated with anti-CD3 for 18-20 hours and transformed with retrovirus expressing EB3-GFP. At day 4 following transformation, T cells were purified and plated on glass bottom dishes coated with anti-CD3 or CD45 antibodies. Live images were taken using the Olympus FV1000 confocal after cells were settled for 15-45 minutes on the dishes. Images of individual cells were obtained every 2 seconds for 3-5 minutes. Microtubule growth rate measurements were generated using the MTrackJ plugin for ImageJ. Statistical analysis was obtained from greater than 50 microtubule tracks from more than 10 cells each from 3 separate experiments.

Results

Inhibition of ERK decreases efficiency of MTOC polarization

ERK was previously shown to be important for cytolysis by CD8 T cells (16) suggesting that it may play a role in T cell polarity. To address this more directly, we tested if the MTOC can polarize in activated T cells when ERK is inhibited, by measuring MTOC polarization in the presence or absence of the MEK inhibitor UO126. Since MEK activation is required for ERK activation, MEK inhibition blocks ERK activation. Mouse T cells were treated with UO126 for one hour and then plated onto anti-CD3 coated coverslips to induce MTOC polarization. Cells were also treated with inhibitors to block actin polymerization (Cytochalasin d) and cAMP (RPcAMP) as positive and negative controls, respectively. After staining with anti-tubulin to visualize the MTOC, the percentage of cells whose MTOC was polarized to the antibody coated surface was measured by confocal microscopy. Cells were scored as polarized if the MTOC was clearly visible in the center of the cell at a focal plane adjacent to the glass coverslip (Figure 1A). We noted a 40–50% decrease in MTOC polarization in the cells treated with MEK inhibitor (Figure 1B), confirming that ERK activity is important for MTOC polarization in T cells.

Stathmin is rapidly phosphorylated downstream of the TCR in an ERK-dependent manner

Recently, it was shown that ERK is recruited to the immunological synapse (14, 15). This suggests that the polarized recruitment of ERK may function to phosphorylate proteins at the synapse that may be important for MTOC polarization. We focused on stathmin because it is a well-known ERK substrate and functions to modulate microtubule dynamics. Therefore, we examined the relationship between ERK and stathmin in the regulation of microtubule dynamics in activated T cells.

We first wanted to confirm that stathmin is phosphorylated by ERK following TCR engagement. To test this, Jurkat T cells were treated with PMA (Fig. 2A) or anti-CD3 (Fig. 2B) for various time points. Immunoblotting of cell lysates with an antibody that recognizes phosphorylated stathmin showed that stathmin is phosphorylated within 15 minutes of stimulation and remains phosphorylated over two hours (Figure 2A, B). This was ERK specific as treatment with the MEK inhibitor UO126 largely abrogated stathmin phosphorylation (Figure 2A, B). This finding was confirmed in primary T cells stimulated with peptide-loaded APCs (Figure 2C and data not shown). Together, these data demonstrate that stathmin is phosphorylated in an ERK-dependent manner downstream of the TCR.

Phosphorylated stathmin is enriched at the immune synapse of primary CTL

To determine whether phosphorylated stathmin localizes to the immunological synapse, antibodies to phosphostathmin were used to stain TCR transgenic primary T cells conjugated with peptide-coated APCs. This demonstrated a clear accumulation of phospho-stathmin at the immune synapse in approximately 72% of conjugates (Figure 2C and Figure 3). Interestingly, no specific enrichment was seen using an antibody that recognizes all stathmin molecules (Figure 2D). This suggests that the recruitment of ERK to the synapse allows for local phosphorylation of stathmin molecules. Since stathmin is a cytoplasmic molecule, phosphorylation is likely to be dynamic resulting in the continuous release of microtubule subunits (34). This suggests that polarized stathmin phosphorylation might be important in the regulation of microtubule dynamics at the immune synapse during T cell activation.

Synapse localization of phosphorylated stathmin is disrupted in KSR1−/− T cells

We previously showed that the scaffold molecule KSR1 facilitates the localization of phosphorylated ERK (pERK) at the immunological synapse (14). We could therefore use KSR1-deficient cells to confirm whether the localization of pERK at the immunological synapse was involved in polarized stathmin phosphorylation. Cell conjugates generated using wild-type or knockout KSR1 TCR transgenic T cells and peptide-pulsed APCs were stained with phospho-stathmin antibodies As expected, phospho-stathmin was localized at the immune synapse of wild-type cells, but phospho-stathmin polarization was significantly decreased in KSR1-deficient T cells (Figure 3). This supports the idea that KSR1-dependent recruitment of phospho-ERK to the immune synapse allows for polarized phosphorylation of stathmin at the immune synapse.

T cells from stathmin−/− mice have defects in MTOC polarization and CTL cytolysis

To confirm that stathmin was involved in MTOC polarization, we assessed MTOC polarization in T cells from wild-type and stathmin deficient mice to anti-CD3 coated coverslips. We observed an approximately 50% decrease in MTOC polarization in stathmin knockout T cells compared to wild-type T cells at multiple time points (Figure 4A). To extend these findings to a more physiologic assay, we assessed MTOC polarization in APC conjugates with wild-type or stathmin knockout T cells (Figure 4B). Consistent with our data from anti-CD3 coated coverslips, we observed a significant decrease in MTOC polarization after 5 minutes in stathmin knockout T cells compared to wild type. These data support a role for stathmin in regulating MTOC reorientation during T cell activation.

To determine whether the defect in MTOC polarization in stathmin-deficient T cells was physiologically significant, we performed a number of assays of T cell function. Because MTOC polarization is required for efficient cytolysis by CD8 T cells, we first tested whether stathmin knockout CTLs were defective in cytolysis. Indeed, CTL generated from stathmin deficient animals demonstrated a defect in specific lysis of peptide-loaded targets using a conventional Cr^{51}-release assay (Figure 4C). To determine whether stathmin knockout T cells were defective in degranulation, we also measured surface LAMP-1 staining during a 45-minute incubation with target cells (Figure 4D, E). We found that the magnitude of degranulation as measured by LAMP-1 staining was lower in stathmin deficient cells compared to wild-type cells (Figure 4E). The basal level of LAMP-1 staining was however, higher in stathmin deficient cells suggesting constitutive non-specific degranulation in these cells (Figure 4D). This data supports the idea that stathmin is involved in MTOC polarization and cytolysis by CD8+ T cells. Surprisingly, stathmin knockout T cells performed normally in other assays of T cell function we performed, including proliferation and migration (Figure 5A and B). Stathmin knockout T cells also produced similar levels of IFN-γ compared to wild-type T cells (Figure 5C).

T cells from stathmin−/− mice have impaired PKCθ polarization and microtubule dynamics

Our data suggest that ERK phosphorylates stathmin at the immune synapse following T cell activation and that this leads to the dynamic restructuring of the microtubule network facilitating MTOC polarization. It is possible, however, that defects in TCR proximal signaling, rather than defects in microtubule dynamics, contribute to the MTOC polarization defect we observed in stathmin deficient cells. To rule out this possibility, we first tested whether conjugate formation was affected in the absence of stathmin. No differences between wild-type and stathmin deficient T cells was seen (data not shown). In addition, activation of ERK and PLC-γ was normal in stathmin-deficient T cells (Figure 6A). Lastly, stathmin deficient T cells also fluxed calcium at wild-type levels (Figure 6B). This suggests that proximal TCR signaling is intact in stathmin knockout T cells.

Since PKCθ polarization was previously shown to precede MTOC polarization in T cells (12), we also assessed PKCθ polarization in stathmin knockout T cells. T cell conjugates were generated and stained using antibodies to PKCθ. We found that there was a defect in PKCθ polarization in stathmin-deficient T cells as compared to wild-type cells (Figure 6C). While PLC-γ is known to control PKCθ recruitment to the immunological synapse (12), we did not detect defects in PLC-γ activation in stathmin-deficient T cells (Figure 6A). Therefore, it seems unlikely that a defect in diacylglycerol (DAG) production is the cause of the PKCθ polarization defect, though we did not directly measure DAG accumulation at the synapse and therefore cannot completely rule out this possibility. Our data suggests, however, that PKCθ polarization may depend on an intact microtubule network. Consistent with this, we found that nocodazole-mediated disruption of microtubules in T cells blocked PKCθ polarization (data not shown).

Since defects in early TCR signaling are probably not responsible for the MTOC polarization defects in stathmin-deficient T cells, we directly tested whether stathmin plays a role in microtubule dynamics by measuring microtubule dynamics in T cells stimulated with anti-CD3 or a control antibody (CD45). To label microtubules, we transduced cells with a GFP fusion protein of EB3, a protein that binds to the ends of growing microtubules (35). Using real-time confocal microscopy, we found that T cell activation strongly enhanced microtubule growth rate with microtubules in activated cells moving at a growth rate of about 50% greater than cells plated on the control antibody (Figure 6D). This enhancement appeared to require stathmin as the microtubule growth rate in stathmin deficient T cells was much slower compared to wild-type T cells (Figure 6D). These data support a role for phosphorylated stathmin in regulating microtubule growth in activated T cells, MTOC polarization and cytolysis by CD8+ T cells.

Discussion

Here we showed that the localization of ERK to the immunological synapse plays a role in T cell polarization. By using T cells deficient in KSR1, a scaffolding molecule required for ERK localization at the synapse, we were able to correlate the loss of polarized ERK localization with defective polarized stathmin phosphorylation. This supports the idea that the retention of activated ERK at the synapse allows it to phosphorylate specific substrates at the synapse in a polarized fashion. We suspect that the localized phosphorylation of ERK substrates may play a role in T cell polarization.

We began our studies by trying to identify a specific ERK substrate at the immunological synapse. Given the critical role of MTOC polarization in T cell polarity, we searched for an ERK substrate that might be a regulator of the microtubule cytoskeleton. This led us to examine stathmin, a known ERK substrate and microtubule regulator (19, 21, 22, 24). Stathmin functions by binding to tubulin αβ heterodimers, sequestering them and preventing them from being assembled into microtubules (36). Since microtubule assembly is critically dependent on the concentration of free tubulin heterodimers (37), the localized release of tubulin is likely to play an important role in localized assembly and growth of microtubules. Consistent with this hypothesis, we showed that microtubule growth was strongly enhanced by T cell activation in a mechanism that was ERK and stathmin dependent. To our knowledge, our studies are the first to show that T cell activation enhances the growth rate of microtubule movement. It seems reasonable to speculate that an increased rate of microtubule growth at the immunological synapse may play a role in repositioning of the MTOC.

Previously, it was shown that mice lacking stathmin demonstrate decreased thymocyte and peripheral cell numbers suggesting an important role for stathmin in T lymphocyte function,

however no other T lymphocyte abnormality was reported (30). Here we found that T cells lacking stathmin showed decreased PKCθ polarization, delayed MTOC polarization, decreased microtubule growth rates and moderate defects in CTL killing, as well as decreased antigen-induced degranulation due to increased basal degranulation. Surprisingly, we did not detect any other defects in T cell function, including proliferation, migration, conjugate formation (data not shown), immune synapse formation (data not shown), and cytokine release. While this might suggest that there are compensatory pathways activated in the absence of stathmin, we were unable to detect mRNA expression of other stathmin family proteins (RB3, SCLIP and SGC10) in either wild-type or knockout mice (data not shown) suggesting that there is not a compensatory increase in expression of other stathmin family members.

Given the importance of MTOC reorientation in directing T cell polarity and polarized intracellular trafficking and secretion (4, 7), it is surprising that the role of microtubules during T cell activation is relatively unexplored. This may be due to previous studies that showed that TCR signaling, proliferation and cytolysis are largely unaffected by treatment with drugs that inhibit microtubules (38–40). Given that these inhibitors profoundly inhibit T cell polarization, our results suggest that role of microtubules in T cell activation be reexamined in more physiological situations. We found, for example, that nocodazole treatment blocked MTOC polarization and also inhibited PLC-γ (data not shown). This could also explain some of the inconsistencies in the literature regarding the role of microtubules (41, 42). Nevertheless, our results suggest that microtubule regulation is an important aspect of T cell activation.

Our work also implicates the ERK MAP kinase pathway as playing an important role in regulating cell polarity. One function of the immunological synapse may be to help the assembly of a signaling apparatus that directs the reorientation of the cell. It is interesting to speculate that the effects of DAG on cell polarization (10) may be related to the ability of DAG to activate the RAS/MAPK signaling pathway via the activation of RASGRP (13). Since DAG is constrained to the plasma membrane and can be quickly inactivated by lipid kinases (43), Ras activation occurs in a localized fashion in the immunological synapse. Previously, we showed that the recruitment of the scaffold KSR1 to the immunological synapse functions to tether and hold activated ERK at the synapse (14). In the absence of KSR1, we speculated that activated ERK would diffuse away from the synapse and into the cytoplasm. Our work suggests that holding ERK at the synapse may function to allow it to phosphorylate specific substrates involved in cell polarization, such as stathmin. Given that ERK can phosphorylate a wide variety of different proteins, it seems likely that stathmin might not be the only protein phosphorylated by ERK involved in cell polarity. The challenge for the immediate future will be to identify these other substrates.

Acknowledgments

We would like to thank Dr. U. K. Schubart and Dr. G. P. Shumyatsky for kindly providing stathmin1−/− mice. This work was supported by the NIH (R37-AI57966-AS and T32-AI07163-EF) and the Howard Hughes Medical Institute.

References

1. Grakoui A, Bromley SK, Sumen C, Davis MM, Shaw AS, Allen PM, Dustin ML. The immunological synapse: a molecular machine controlling T cell activation. Science. 1999; 285:221–227. [PubMed: 10398592]
2. Kupfer A, Dennert G, Singer SJ. Polarization of the Golgi apparatus and the microtubule-organizing center within cloned natural killer cells bound to their targets. Proc Natl Acad Sci U S A. 1983; 80:7224–7228. [PubMed: 6359165]

3. Kuhn JR, Poenie M. Dynamic polarization of the microtubule cytoskeleton during CTL-mediated killing. Immunity. 2002; 16:111–121. [PubMed: 11825570]
4. Stinchcombe JC, Majorovits E, Bossi G, Fuller S, Griffiths GM. Centrosome polarization delivers secretory granules to the immunological synapse. Nature. 2006; 443:462–465. [PubMed: 17006514]
5. Kupfer A, Dennert G. Reorientation of the microtubule-organizing center and the Golgi apparatus in cloned cytotoxic lymphocytes triggered by binding to lysable target cells. J Immunol. 1984; 133:2762–2766. [PubMed: 6384372]
6. Stinchcombe JC, Bossi G, Booth S, Griffiths GM. The immunological synapse of CTL contains a secretory domain and membrane bridges. Immunity. 2001; 15:751–761. [PubMed: 11728337]
7. Huse M, Lillemeier BF, Kuhns MS, Chen DS, Davis MM. T cells use two directionally distinct pathways for cytokine secretion. Nat Immunol. 2006; 7:247–255. [PubMed: 16444260]
8. Lowin-Kropf B V, Shapiro S, Weiss A. Cytoskeletal polarization of T cells is regulated by an immunoreceptor tyrosine-based activation motif-dependent mechanism. J Cell Biol. 1998; 140:861–871. [PubMed: 9472038]
9. Kuhne MR, Lin J, Yablonski D, Mollenauer MN, Ehrlich LI, Huppa J, Davis MM, Weiss A. Linker for activation of T cells, zeta-associated protein-70, and Src homology 2 domain-containing leukocyte protein-76 are required for TCR-induced microtubule-organizing center polarization. J Immunol. 2003; 171:860–866. [PubMed: 12847255]
10. Quann EJ, Merino E, Furuta T, Huse M. Localized diacylglycerol drives the polarization of the microtubule-organizing center in T cells. Nat Immunol. 2009; 10:627–635. [PubMed: 19430478]
11. Robertson LK, Mireau LR, Ostergaard HL. A role for phosphatidylinositol 3-kinase in TCR-stimulated ERK activation leading to paxillin phosphorylation and CTL degranulation. J Immunol. 2005; 175:8138–8145. [PubMed: 16339552]
12. Quann EJ, Liu X, Altan-Bonnet G, Huse M. A cascade of protein kinase C isozymes promotes cytoskeletal polarization in T cells. Nat Immunol. 12:647–654. [PubMed: 21602810]
13. Ebinu JO, Stang SL, Teixeira C, Bottorff DA, Hooton J, Blumberg PM, Barry M, Bleakley RC, Ostergaard HL, Stone JC. RasGRP links T-cell receptor signaling to Ras. Blood. 2000; 95:3199–3203. [PubMed: 10807788]
14. Giurisato E, Lin J, Harding A, Cerutti E, Cella M, Lewis RE, Colonna M, Shaw AS. The mitogen-activated protein kinase scaffold KSR1 is required for recruitment of extracellular signal-regulated kinase to the immunological synapse. Mol Cell Biol. 2009; 29:1554–1564. [PubMed: 19139278]
15. Yachi PP, Ampudia J, Zal T, Gascoigne NR. Altered peptide ligands induce delayed CD8-T cell receptor interaction--a role for CD8 in distinguishing antigen quality. Immunity. 2006; 25:203–211. [PubMed: 16872849]
16. Lilic M, Kulig K, Messaoudi I, Remus K, Jankovic M, Nikolic-Zugic J, Vukmanovic S. CD8(+) T cell cytolytic activity independent of mitogen-activated protein kinase / extracellular regulatory kinase signaling (MAP kinase / ERK). Eur J Immunol. 1999; 29:3971–3977. [PubMed: 10602006]
17. Chen X, Allan DS, Krzewski K, Ge B, Kopcow H, Strominger JL. CD28-stimulated ERK2 phosphorylation is required for polarization of the microtubule organizing center and granules in YTS NK cells. Proc Natl Acad Sci U S A. 2006; 103:10346–10351. [PubMed: 16801532]
18. Nejmeddine M V, Negi S, Mukherjee S, Tanaka Y, Orth K, Taylor GP, Bangham CR. HTLV-1-Tax and ICAM-1 act on T-cell signal pathways to polarize the microtubule-organizing center at the virological synapse. Blood. 2009; 114:1016–1025. [PubMed: 19494354]
19. Di Paolo G, Antonsson B, Kassel D, Riederer BM, Grenningloh G. Phosphorylation regulates the microtubule-destabilizing activity of stathmin and its interaction with tubulin. FEBS Lett. 1997; 416:149–152. [PubMed: 9369201]
20. Lovric J, Dammeier S, Kieser A, Mischak H, Kolch W. Activated raf induces the hyperphosphorylation of stathmin and the reorganization of the microtubule network. J Biol Chem. 1998; 273:22848–22855. [PubMed: 9712920]
21. Burkhard KA, Chen F, Shapiro P. Quantitative analysis of ERK2 interactions with substrate proteins: roles for kinase docking domains and activity in determining binding affinity. J Biol Chem. 286:2477–2485. [PubMed: 21098038]

22. Marklund U, Brattsand G, Shingler V, Gullberg M. Serine 25 of oncoprotein 18 is a major cytosolic target for the mitogen-activated protein kinase. J Biol Chem. 1993; 268:15039–15047. [PubMed: 8325880]
23. Leighton IA, Curmi P, Campbell DG, Cohen P, Sobel A. The phosphorylation of stathmin by MAP kinase. Mol Cell Biochem. 1993; 127–128:151–156.
24. Curmi PA, Gavet O, Charbaut E, Ozon S, Lachkar-Colmerauer S, Manceau V, Siavoshian S, Maucuer A, Sobel A. Stathmin and its phosphoprotein family: general properties, biochemical and functional interaction with tubulin. Cell Struct Funct. 1999; 24:345–357. [PubMed: 15216892]
25. Melhem RF, Zhu XX, Hailat N, Strahler JR, Hanash SM. Characterization of the gene for a proliferation-related phosphoprotein (oncoprotein 18) expressed in high amounts in acute leukemia. J Biol Chem. 1991; 266:17747–17753. [PubMed: 1917919]
26. Gratiot-Deans J, Keim D, Strahler JR, Turka LA, Hanash S. Differential expression of Op18 phosphoprotein during human thymocyte maturation. J Clin Invest. 1992; 90:1576–1581. [PubMed: 1401087]
27. Wang YK, Liao PC, Allison J, Gage DA, Andrews PC, Lubman DM, Hanash SM, Strahler JR. Phorbol 12-myristate 13-acetate-induced phosphorylation of Op18 in Jurkat T cells. Identification of phosphorylation sites by matrix-assisted laser desorption ionization mass spectrometry. J Biol Chem. 1993; 268:14269–14277. [PubMed: 8314790]
28. le Gouvello S, Chneiweiss H, Tarantino N, Debre P, Sobel A. Stathmin phosphorylation patterns discriminate between distinct transduction pathways of human T lymphocyte activation through CD2 triggering. FEBS Lett. 1991; 287:80–84. [PubMed: 1679022]
29. le Gouvello S, Manceau V, Sobel A. Serine 16 of stathmin as a cytosolic target for Ca2+/calmodulin-dependent kinase II after CD2 triggering of human T lymphocytes. J Immunol. 1998; 161:1113–1122. [PubMed: 9686569]
30. Schubart UK, Yu J, Amat JA, Wang Z, Hoffmann MK, Edelmann W. Normal development of mice lacking metablastin (P19), a phosphoprotein implicated in cell cycle regulation. J Biol Chem. 1996; 271:14062–14066. [PubMed: 8662897]
31. Hogquist KA, Jameson SC, Heath WR, Howard JL, Bevan MJ, Carbone FR. T cell receptor antagonist peptides induce positive selection. Cell. 1994; 76:17–27. [PubMed: 8287475]
32. Kaye J, Hsu ML, Sauron ME, Jameson SC, Gascoigne NR, Hedrick SM. Selective development of CD4+ T cells in transgenic mice expressing a class II MHC-restricted antigen receptor. Nature. 1989; 341:746–749. [PubMed: 2571940]
33. Nguyen A, Burack WR, Stock JL, Kortum R, Chaika OV, Afkarian M, Muller WJ, Murphy KM, Morrison DK, Lewis RE, McNeish J, Shaw AS. Kinase suppressor of Ras (KSR) is a scaffold which facilitates mitogen-activated protein kinase activation in vivo. Mol Cell Biol. 2002; 22:3035–3045. [PubMed: 11940661]
34. Blaineau C, Tessier M, Dubessay P, Tasse L, Crobu L, Pages M, Bastien P. A novel microtubule-depolymerizing kinesin involved in length control of a eukaryotic flagellum. Curr Biol. 2007; 17:778–782. [PubMed: 17433682]
35. Stepanova T, Slemmer J, Hoogenraad CC, Lansbergen G, Dortland B, De Zeeuw CI, Grosveld F, van Cappellen G, Akhmanova A, Galjart N. Visualization of microtubule growth in cultured neurons via the use of EB3-GFP (end-binding protein 3-green fluorescent protein). J Neurosci. 2003; 23:2655–2664. [PubMed: 12684451]
36. Larsson N, Segerman B, Howell B, Fridell K, Cassimeris L, Gullberg M. Op18/stathmin mediates multiple region-specific tubulin and microtubule-regulating activities. J Cell Biol. 1999; 146:1289–1302. [PubMed: 10491392]
37. Kirschner M, Mitchison T. Beyond self-assembly: from microtubules to morphogenesis. Cell. 1986; 45:329–342. [PubMed: 3516413]
38. Brown DL, Little JE, Chaly N, Schweitzer I, Paulin-Levasseur M. Effects of taxol on microtubule organization in mouse splenic lymphocytes and on response to mitogenic stimulation. Eur J Cell Biol. 1985; 37:130–139. [PubMed: 2863144]
39. Knox JD, Mitchel RE, Brown DL. Effects of taxol and taxol/hyperthermia treatments on the functional polarization of cytotoxic T lymphocytes. Cell Motil Cytoskeleton. 1993; 24:129–138. [PubMed: 8095001]

40. Dianzani U, Shaw A, Kal-Ramadi B, Kubo RT, Janeway CA Jr. Physical association of CD4 with the T cell receptor. J Immunol. 1992; 148:678–688. [PubMed: 1370513]

41. Huby RD, Weiss A, Ley SC. Nocodazole inhibits signal transduction by the T cell antigen receptor. J Biol Chem. 1998; 273:12024–12031. [PubMed: 9575143]

42. Martin-Cofreces NB, Robles-Valero J, Cabrero JR, Mittelbrunn M, Gordon-Alonso M, Sung CH, Alarcon B, Vazquez J, Sanchez-Madrid F. MTOC translocation modulates IS formation and controls sustained T cell signaling. J Cell Biol. 2008; 182:951–962. [PubMed: 18779373]

43. Zhong XP, Hainey EA, Olenchock BA, Zhao H, Topham MK, Koretzky GA. Regulation of T cell receptor-induced activation of the Ras-ERK pathway by diacylglycerol kinase zeta. J Biol Chem. 2002; 277:31089–31098. [PubMed: 12070163]

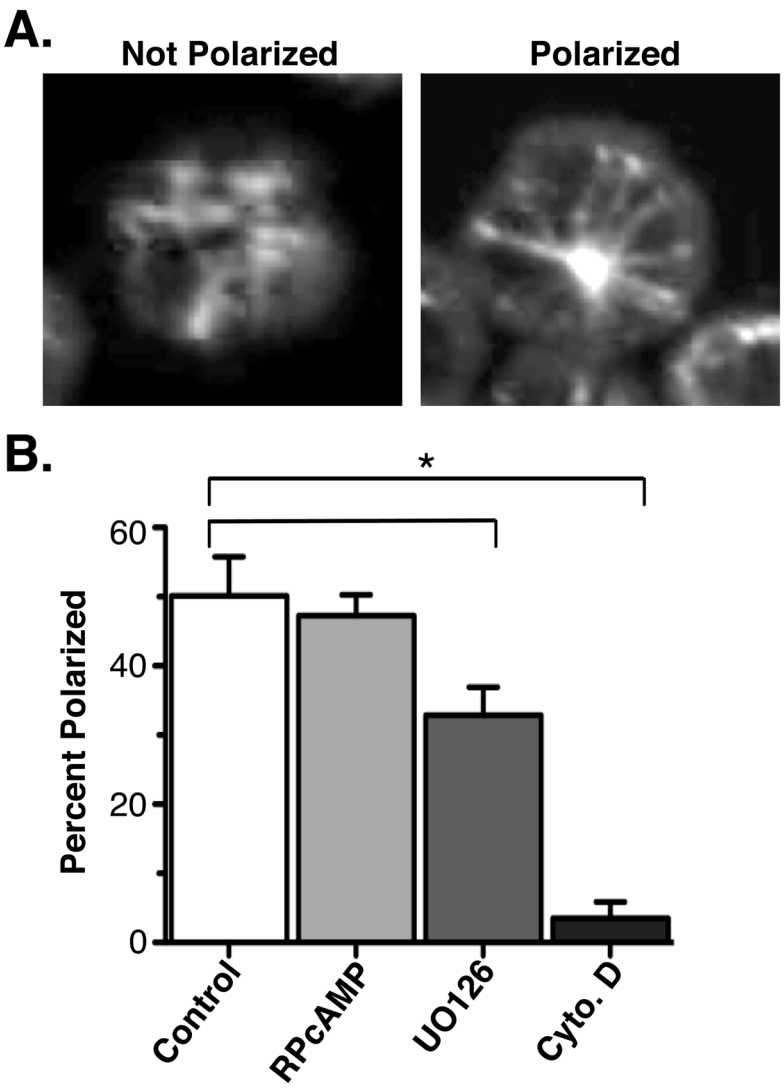

Figure 1. ERK inhibition decreases MTOC polarization in T cells

T cells from B6 mice were pretreated or not for an hour with 0.5μM RPcAMP, 10μM UO126 or 10 μM cytochalasin D and plated on coverslips coated with anti-CD3. Cells were settled for 20 minutes, fixed, permeablized, stained with anti-tubulin and analyzed using confocal microscopy. Images in (A) indicate typical cells scored as polarized and unpolarized. Data in (B) are representative of 4 individual experiments with >50 cells counted per condition per experiment. Error bars show SEM. P value <0.005 (Two-tailed unpaired t-test).

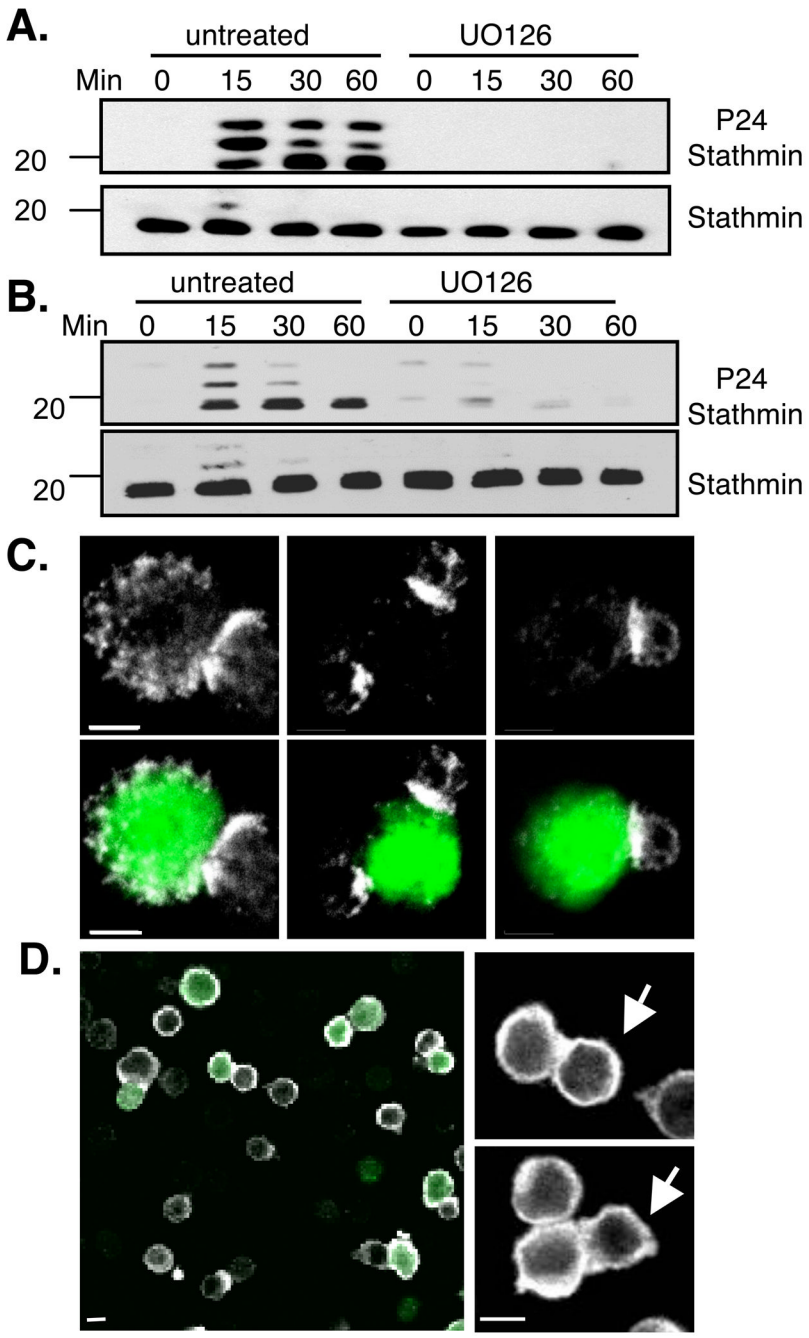

Figure 2. Stathmin is rapidly phosphorylated and accumulates at the immune synapse following TCR engagement in an ERK-dependant manner

Jurkat T cells pretreated or not for 1 hour with 10μM UO126 were stimulated for the indicated time points with 40nM PMA (A) or 1 μg/mL anti-CD3 (B), lysed and resolved on SDS-PAGE gel. Lysates were blotted with antibodies to stathmin or phospho-S24 stathmin. Blots are representative of 4 experiments. (C, D) Spleens from OT-1 mice were stimulated with 1μg SIINFEKL peptide for 5 days until rested. CD8+ T cells were purified and conjugated to either RMA-S or EL4 target cells loaded with peptide and labeled with CFSE (green). Conjugates were stained with stathmin (D) or phosph-S24 (C) antibodies (shown in

white) and analyzed by confocal microscopy. Arrows point to T cells (D). Scale bars = 5μm. Images are representative of >50 conjugates.

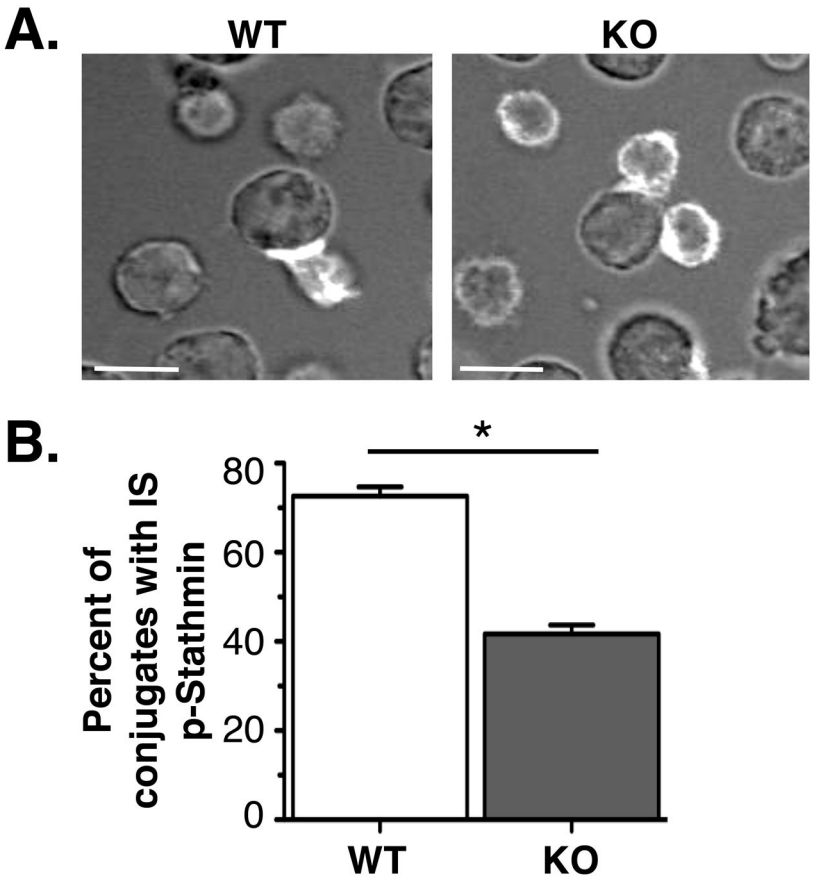

Figure 3. KSR1 is required for immune synapse localization of phosphorylated stathmin

CD4+ T cells from KSR1 wild-type or knockout AND TCR mice were stimulated with CH57 Bcells loaded with 1μg MCC peptide for 5 days until rested. T cells were purified and conjugated with CH27 cells loaded with peptide. Conjugates were stained with phospho-S24 stathminantibody and analyzed by confocal microscopy. (B) Graph represents 3 experiments of >20 conjugates each. Scale bar = 10 μm. P-value <0.001 (Two-tailed unpaired t-test).

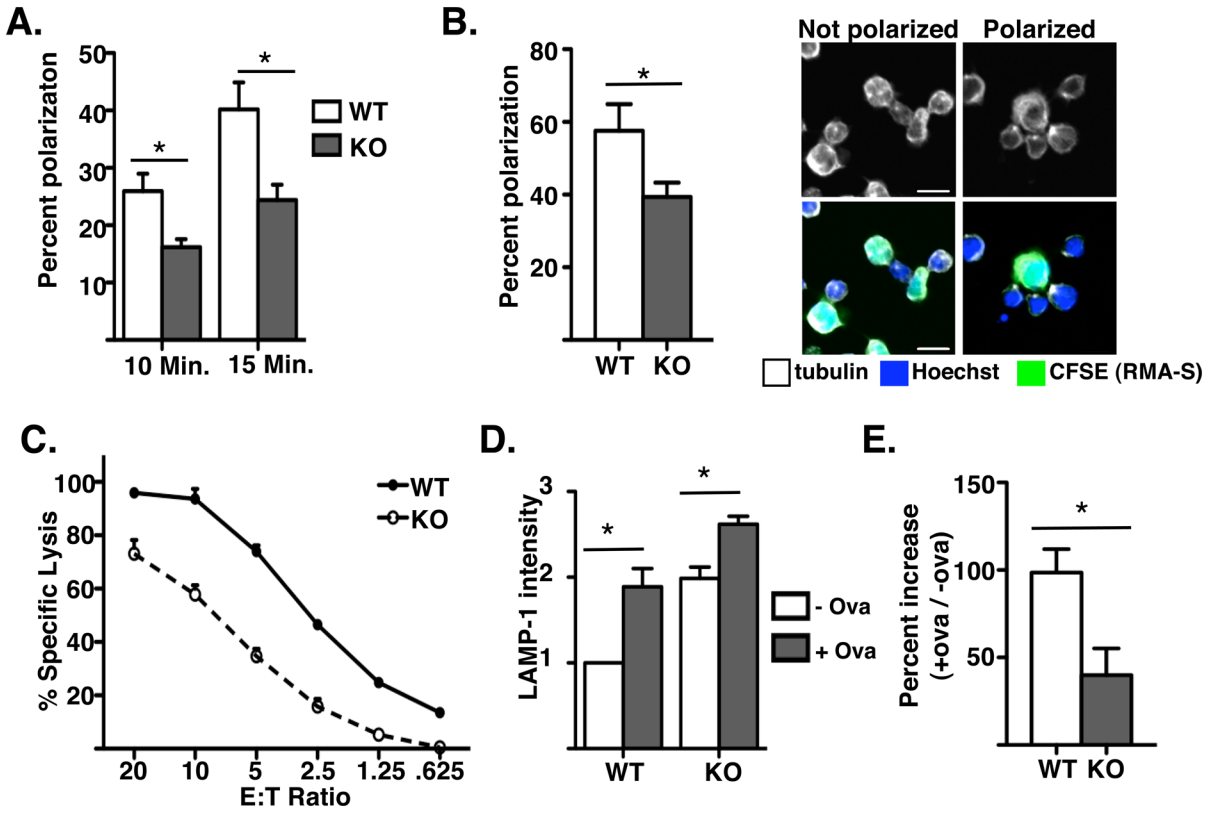

Figure 4. Stathmin−/− T cells have impaired MTOC polarization and are defective in cytolysis

(A) Stathmin knockout or littermate control T cells were purified, rested for 30 minutes and plated on anti-CD3 coated glass coverslips for the indicated time points. Cells were fixed, permeabilized and stained with anti-αβ-tubulin and imaged using confocal microscopy. Data are represented as mean + SEM and more than 50 cells per condition were scored in 3 experiments. All KO values are significantly different from WT ($P<0.001$, Unpaired t test). (B) Rested T cells from stathmin knockout OT-1 or littermate OT-1 controls were conjugated with peptide-pulsed CFSE-labeled RMA-S cells onto glass coverslips for 5 minutes at room temperature. The cells were then fixed, permeabilized, stained with Hoechst and anti-αβ-tubulin, and analyzed using confocal microscopy. Data are represented as mean + SEM and more than 50 cells per condition were scored in 3 experiments. P value < 0.001 (Unpaired t test). Images represent cells scored as polarized or not polarized. Scale bars =10μm. (C) Cytolysis by stathmin KO or littermate control CTL was assayed using standard ^{51}Cr assay. Cells were plated at indicated E:T ratios and incubated for 4–6 hours. Supernatants were counted on a MicroBeta counter and specific lysis was calculated. Differences in specific lysis between stathmin wild-type and knockout CTL are significant ($p<0.001$, Unpaired t-test) at all E:T ratios. Graph is representative of 2 experiments. (D, E) Degranulation was assayed by LAMP-1 staining during 45 minutes of OT-1+ stathmin knockout or control T cell incubation with peptide-loaded RMA-S cells. Graphs show mean + SEM and are representative of 4 experiments.

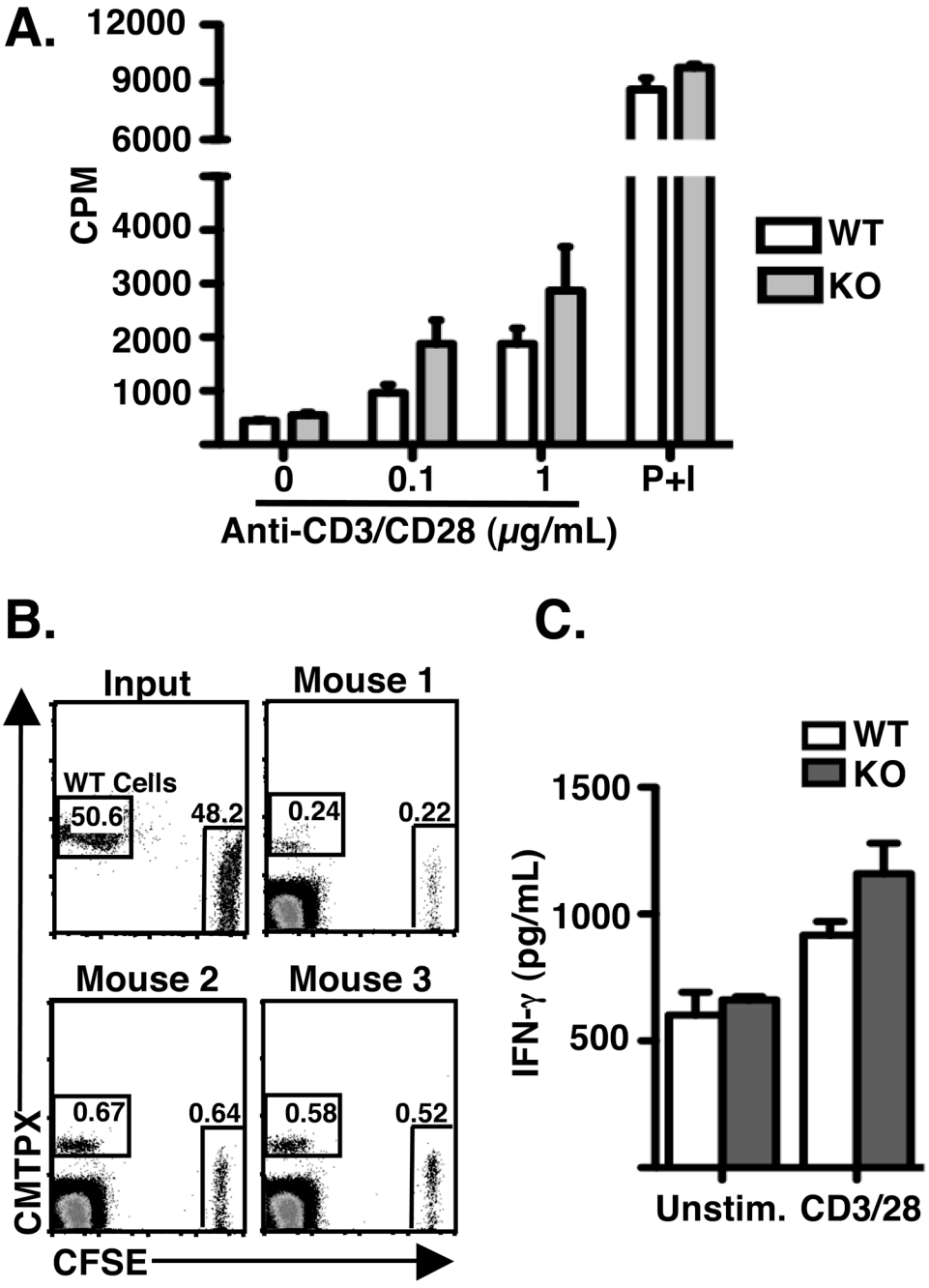

Figure 5. No defect in proliferation, migration and cytokine production of stathmin deficient T cells

(A) Stathmin knockout or littermate control T cells were rested and then restimulated for 48 hours with addition of H^3-Thymidine for the last 16 hours and scintillation counted. Data is presented as mean + SEM and represent 2 experiments. No values are significantly different. (B) Purified T cells from stathmin knockout and control mice were labeled with CFSE and CMTPX, respectively, and injected in a 1:1 ratio into the footpad of LPS-pretreated mice. Cells were harvested and analyzed using flow cytometry after 3 hours. FACS plots are shown from one of two experiments. (C) Rested OT-1 + cells from stathmin knockout or wild type mice were stimulated with 5μg/μL anti-CD3/CD28 for 18 hours and supernatants

were assayed using cytokine bead array. Data is presented as mean + SEM and represent 2 experiments. No values are significantly different.

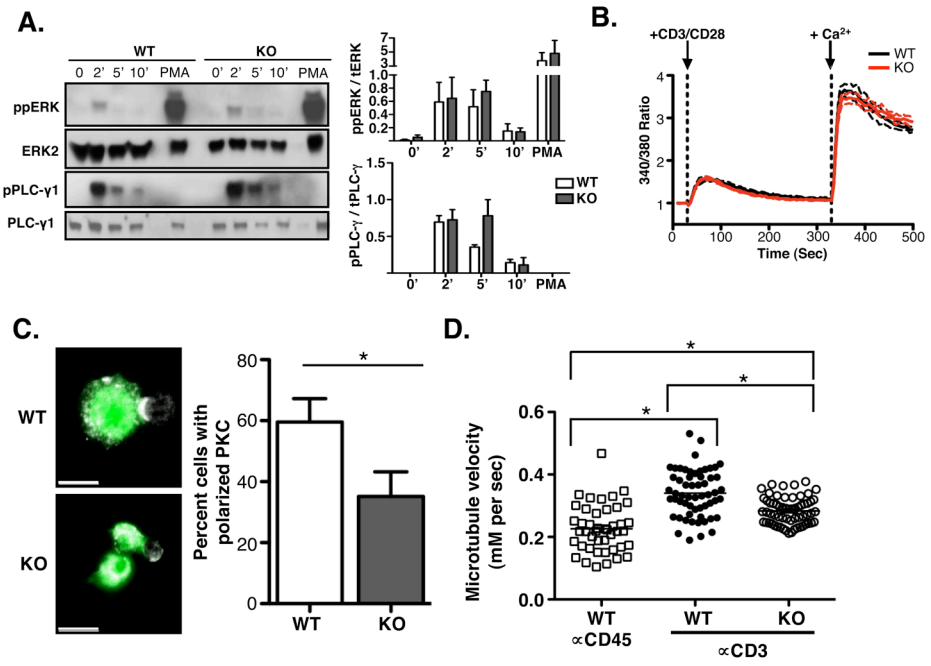

Figure 6. Microtubule growth rate and PKCθ polarization is decreased in stathmin knockout T cells

(A) T cells from stathmin knockout mice or littermate controls were stimulated for the indicated time points with anti-CD3/CD28 or PMA for 10 minutes, lysed and resolved on SDS-PAGE gel. Lysates were blotted with the indicated antibodies. Blots and quantification graphs are representative of 3 experiments. (B) Rested T cells from stathmin knockout or littermate controls were loaded with 1mM Fura and plated in 96-well dishes. Fluorescence ratio between 340 nm and 380 nm excitation at 510 nm emission was recorded. Cells were stimulated after 30 sec with anti-CD3-biot + anti-CD28-biot (5 mg/mL of each) + streptavidin (20 mg/mL), and 1mM $CaCl_2$ was added after 330 sec. Data are represented as mean (solid lines) + SEM (dotted lines) of changes in 340/380 ratio compared with the baseline. Black lines represent stathmin knockout cells and red lines indicated wild-type cells. Graph is representative of 3 experiments. (C) T cells from stathmin wild-type or knockout OT-1 or AND TCR mice were stimulated with peptide pulsed APC for 5 days until rested. T cells were purified, conjugated with peptide pulsed APC and PKCθ antibody and analyzed by confocal microscopy. Graph represents 3 experiments of >50 conjugates each. P-value <0.001 (Two-tailed unpaired t-test). Scale bar = 10μm. (D) Stathmin knockout or littermate control T cells were activated and transformed with a retrovirus expressing EB3-GFP. At day 4 or 5 after activation, cells were plated onto glass bottom dishes and imaged live using confocal microscopy. Microtubule growth rate measurements were generated using MTrackJ. Microtubules were tracked only if they could be followed for 3 or more time-points and if they radiated from the MTOC. Data are from more than 50 microtubules from 10 cells per experiment in 3 individual experiments. * = P< 0.0001 (Mann Whitney test).